Proceedings of the 9th International Conference on Cyclotrons and their Applications
September 1981, Caen, France

STATUS REPORT ON THE 500 MEV CYCLOTRON *

Peter S. Miller and MSU Staff

Cyclotron Laboratory, Michigan State University, East Lansing, MI 48824, USA

Abstract.-The status of the K500 cyclotron construction is reviewed as of August 1981. The first operating tests are anticipated in two months.

1. Introduction.-The assembly of the K500 cyclotron will soon be carried far enough to allow testing with internal beam. The accompanying figures illustrate the progress that is being made.

2. Discussion.The conceptual design of the cyclotron systems is unchanged from that reviewed in the 1978 Conference, but many details have been modified as guided by prototype testing.[1] An example is the rf resonator which was assembled in a test vacuum chamber with a simulated dee electrode and was run at full power to verify the capability for maintaining 100 kV for extended periods. To achieve this it was necessary to modify the sliding shorts so that the contacts are positively clamped when rf is applied.

The 3 rf transmitters are at present under test using 50 kW water loads to simulate the resonators which are being assembled on the magnet.

The copper liners for both poles are installed and are vacuum tight. The coaxial resonators are being installed and leak-checked. The completion of the beam vacuum chamber, i.e. assembly of cryostat, liners and resonators on the magnet is expected by early September. The cryolines for the cryopumps in the dees are installed in the dee stems.

The superconducting coil was removed from its cryostat in early 1980 in order to install the median plane penetrations through the coil bobbin and the cryostat. These penetrations serve the electrostatic deflectors, the magnetic channels, the beam probe and the beam extraction path. The aluminum radiation shield was replaced with one of new design which has improved nitrogen cooling to the upper portions reduces the temperature there to about 80 K as desired. The total heat leak to the coil is close to what it was before these modifications were done.

The inner wall of the cryostat, made of mild steel except near the median plane, is the cyclotron vacuum wall. It was nickel-plated to prevent rust and to reduce the gas load on the pumps.

The magnetic field was mapped in 1980 to determine the details of the iron-produced field. The focusing and phase characteristics of a number of representative ions were calculated, and several iron shims were designed to optimize the performance of the cyclotron. These calculations took note of the expected effect of drilling 156 holes for trim coil leads and 18 others for rf and vacuum components. After these holes were drilled, the trim coils and the magnetic extraction elements were installed and the field mapping was repeated with the final iron configurations. The results agree with the calculations mentioned above.

The power supplies for the main magnet coils are being modified to increase the long-term stability of the currents and to make them compatible with the computer control system. The control system for the cyclotron is CAMAC - based and employs a low speed autopolling network designed and built at MSU to lower costs by creating a buss for each CAMAC slot to increase the number of devices served. The controls and readings from all components in the cyclotron and experimental equipment will be integrated in the system.

The operator controls the cyclotron through two linked computers using a combination of fixed function and multiplexed knobs, switches and displays. The values of interest to the operator are read by the computers and displayed on meters, digital registers, lights or on a television monitor. The system is presently operating with the beam probe, trim coils and harmonic coils connected to it.

*This material is supported by the NSF under Grant No. PHY 80-17605.

References

1. H.G. Blosser, IEEE Trans. on Nucl. Sci. NS-26, No. 2 (1979) 2040.

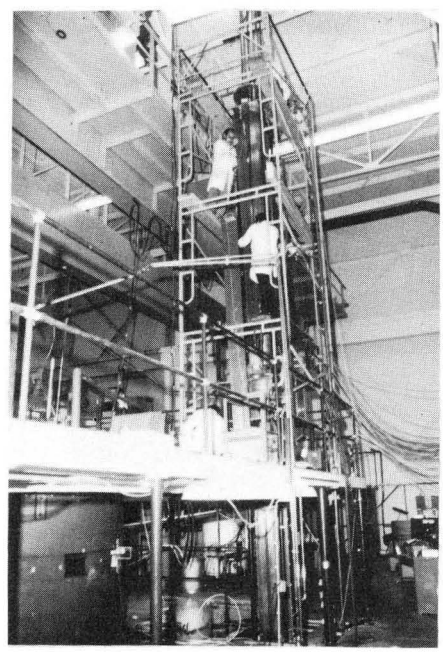

Fig.1: View of the rf test resonator. Most of the upper stem and part of the lower stem are visible. The dee is in a circular aluminum vacuum chamber partly visible through the railing near the center. One of the copper panels of the outer conductor is being installed by the workers.

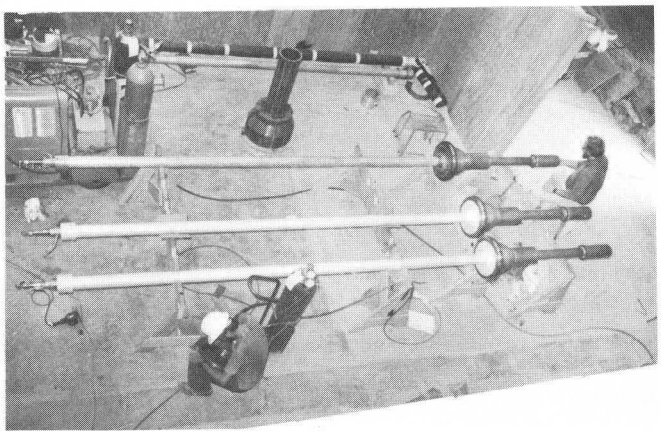

Fig. 2: Dee stem inner conductors in assembly area being fitted for installation. The enlargement of the stem diameter accommodates the insulator, which provides rigid support close to the dee.

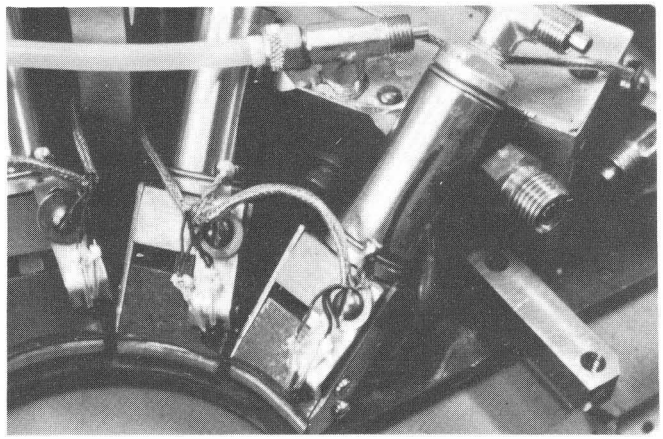

Fig. 5: Spring contacts and clamping mechanism for sliding short on dee stem. The air cylinders force the springs at the lower left against the inner conductor of the coaxial resonator. Phototransistors near the springs detect sparking in case of contact failure and shut off rf.

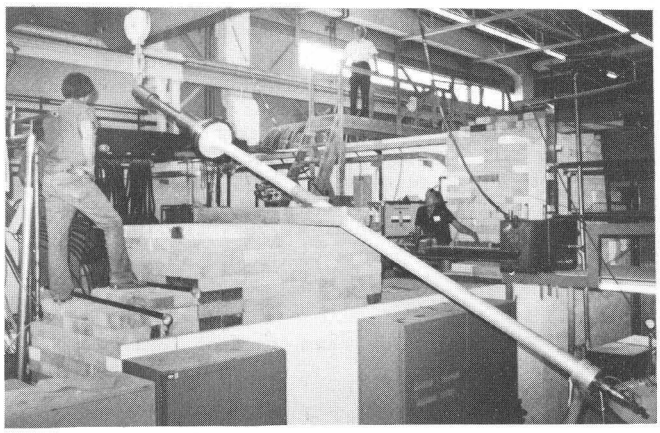

Fig. 3: A stage in the installation of the first dee stem inner conductor. The stem is being pivoted to a vertical position to allow it to be lowered to the pit below the cyclotron.

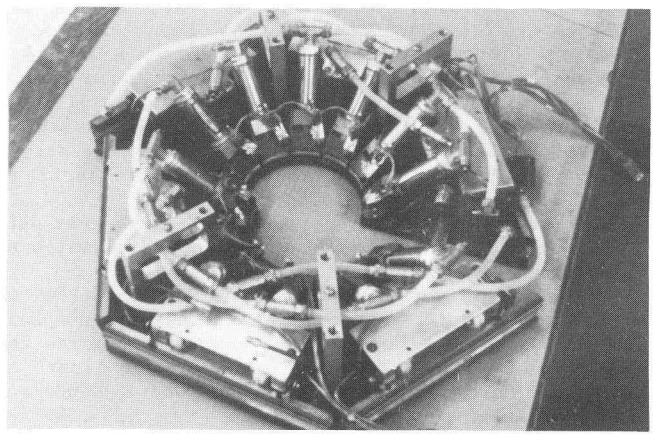

Fig. 6: Sliding short for dee stem. Contacts are clamped to the inner conductor (circular) and the outer conductor (hexagonal) by air cylinders.

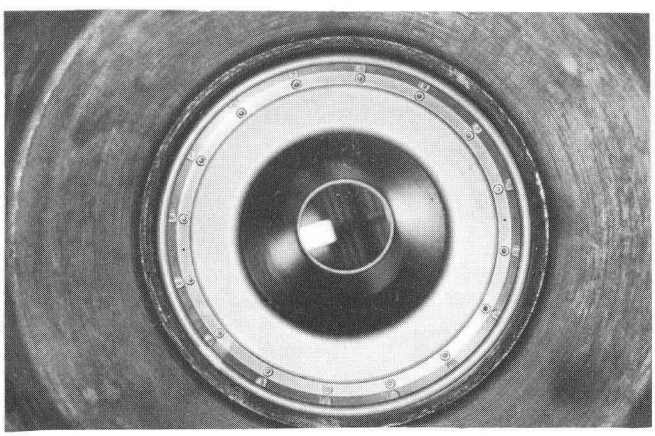

Fig. 4: View into one of the dee stem holes through the lower pole cap, lined with copper. The highly polished interior is in the beam vacuum space; the alumina dee stem insulator fits over the corona ring visible just outside the circle of bolts.

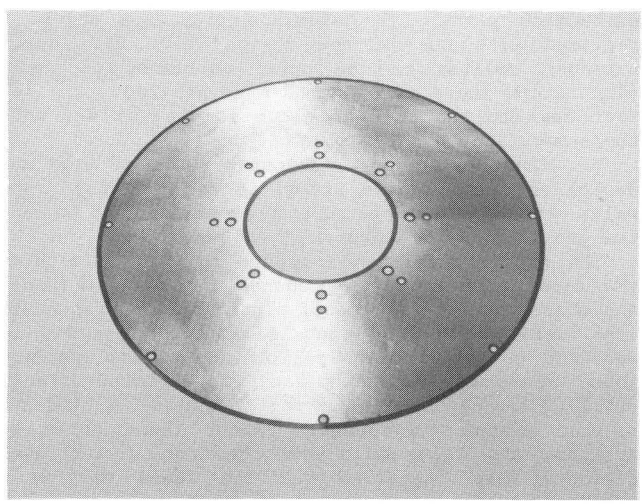

Fig. 7: The screen grid bypass capacitor used in the K500 and K800 transmitters etched from double sided copper clad 5 mil Kapton film. The complete .09μF capacitor contains 2 disks and is vacuum impregnated with silicone rubber.

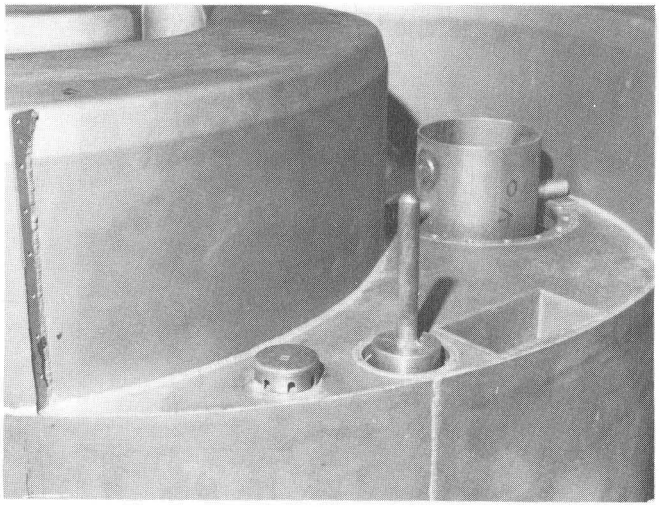

Fig. 8: Rf coupler and dee tuner location seen in a valley of the lower pole. The vertical post is part of the variable capacitor for coupling the rf power to the dee.

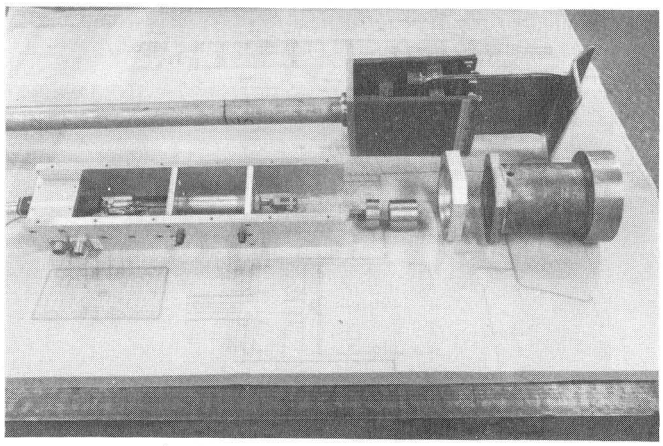

Fig. 9: Dee fine tuner (trimmer capacitor) with hydraulic drive.

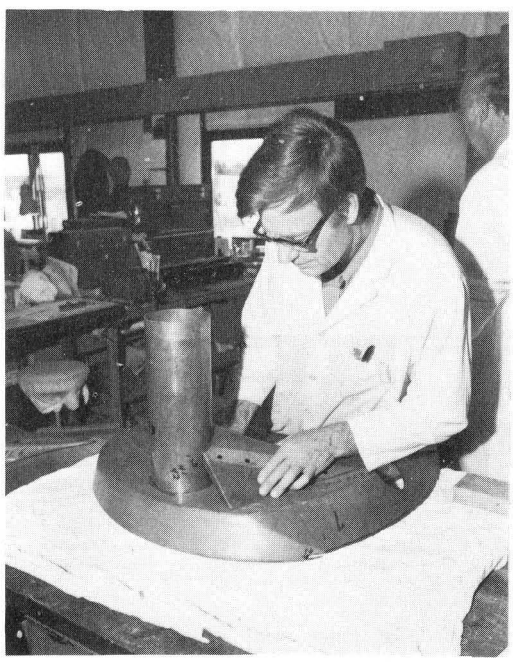

Fig. 10: Fabrication of dees.

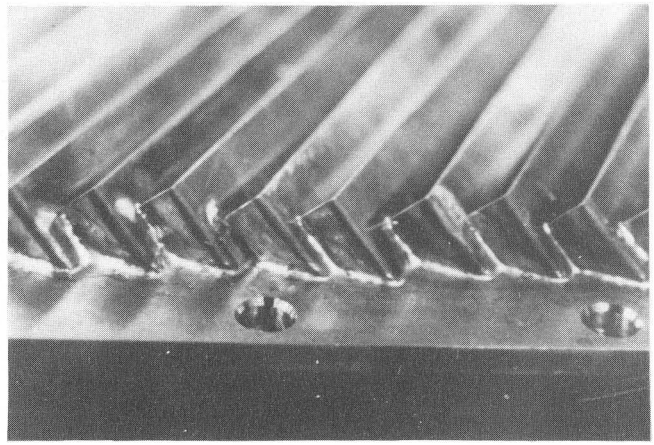

Fig. 11: Close-up view of the liquid nitrogen - temperature baffle surrounding a helium cryopanel located inside a dee.

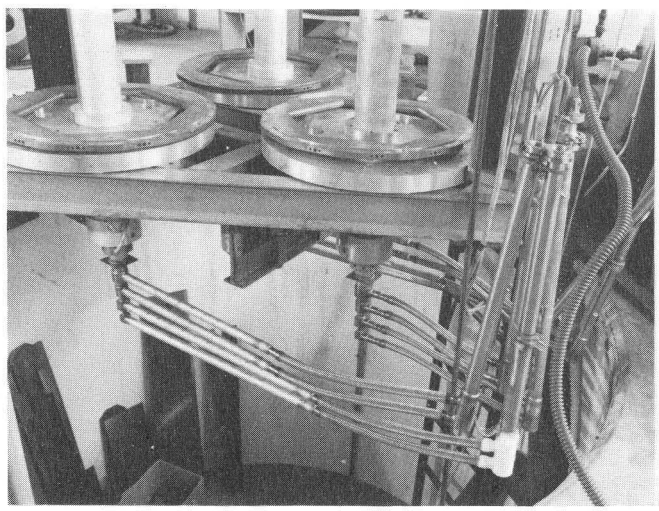

Fig. 12: Cryolines for vacuum pump in lower dee stems. Liquid nitrogen and liquid helium passages inside the dee stem are coaxial with vacuum and superinsulation between all pipes.

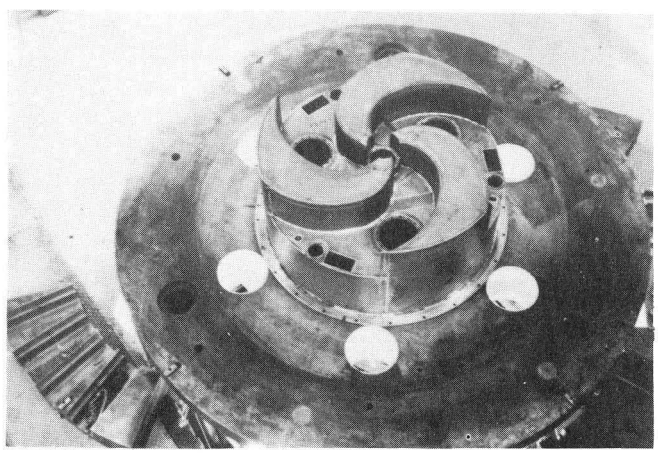

Fig. 13: Lower pole cap with copper rf liner in place over the lower pole. In each valley there is a large hole for the dee stem, a rectangular hole for the dee fine tuner, and adjacent holes for rf coupling capacitor and water lines.

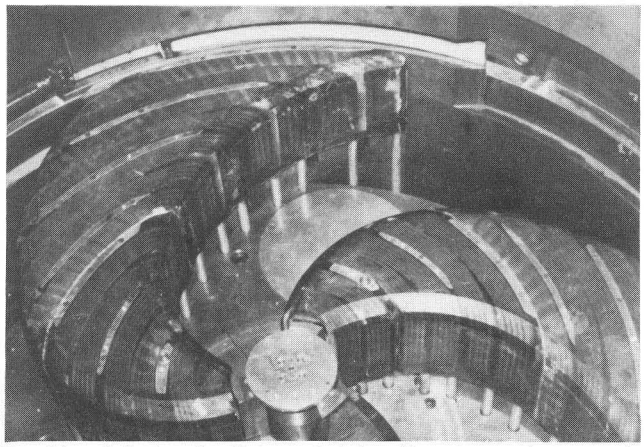

Fig. 14: Spiral pole tips containing the epoxy -impregnated trim coil windings installed in the magnet.

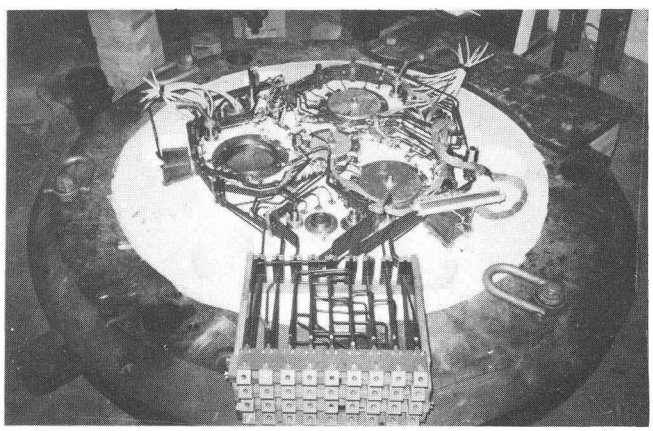

Fig. 15: Electrical and water connections for the trim coils on the outside surface of the pole cap. The 4 rows of 9 terminals each are brass electrical terminals attached to insulating (epoxy-fiberglass) water manifolds.

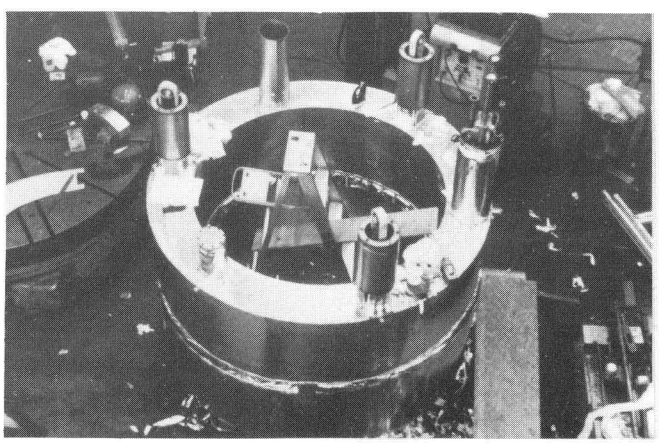

Fig. 16: Aluminum radiation shield (80K) installed on the superconducting coil.

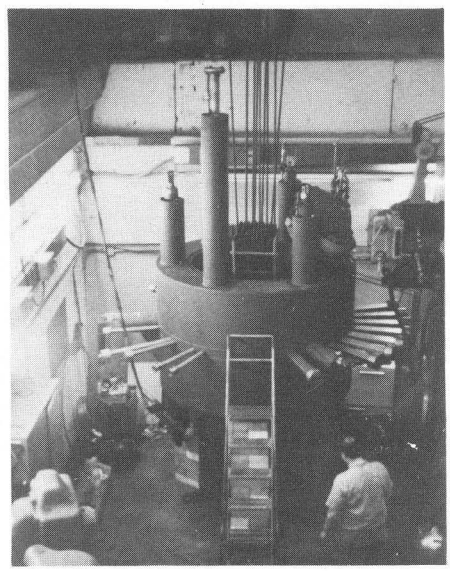

Fig. 17: View of the main coil cryostat showing a number of the median plane penetrations for extraction elements. The tubes extend to the outside of the magnet yoke.

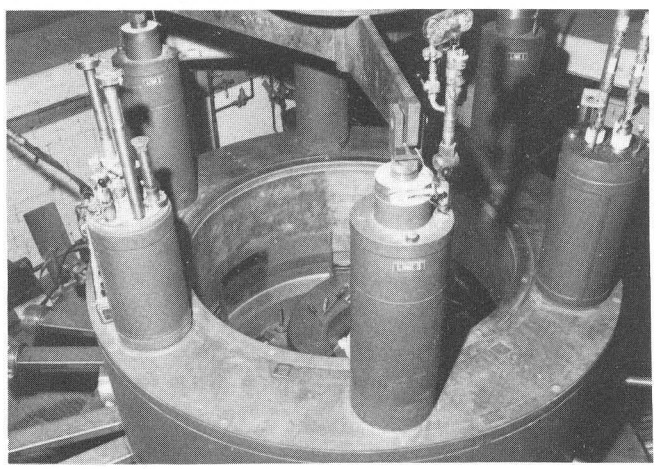

Fig. 18: Cryostat with rf valley liners installed being fitted to the lower pole. The valley liners cover the cryostat wall. One is visible behind cryostat tower marked "LINK 3".

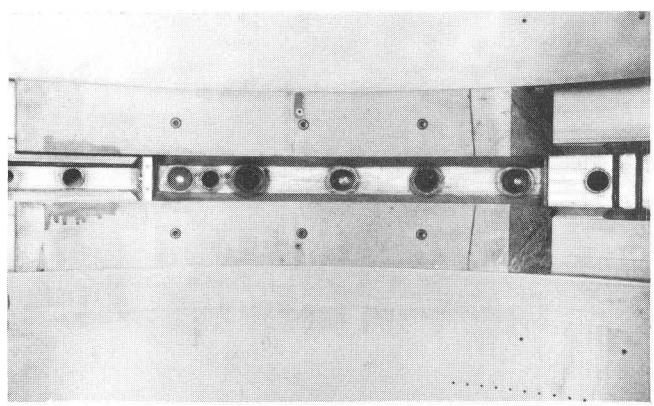

Fig. 19: The inner wall of the nickel-plated cryostat containing spaces for magnetic channel M1 (at left) electrostatic deflector E2 (center) and viewing port at right.

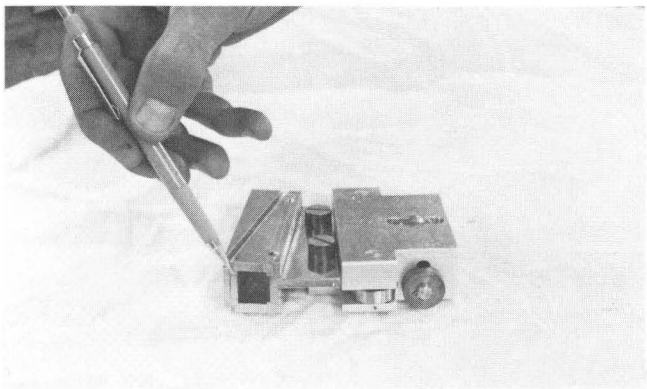

Fig. 20: View into the aperture of one of the focusing bar assemblies. The iron bars are welded into a stainless steel box and the entire assembly is nickel-plated.

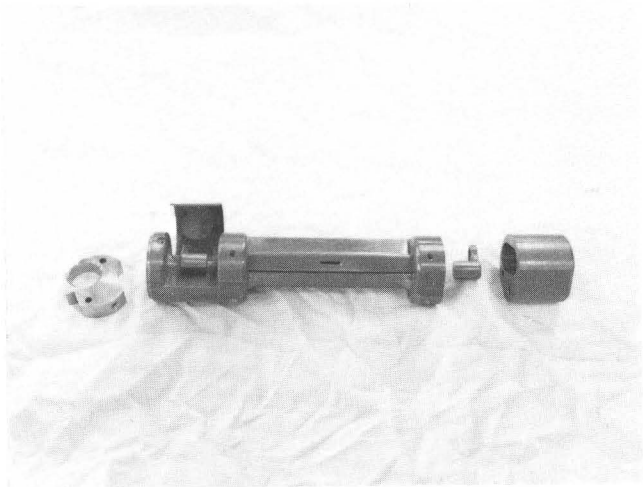

Fig. 21: The PIG ion source is non-magnetic and fits in a 2-inch diameter hole in the center of the magnet.

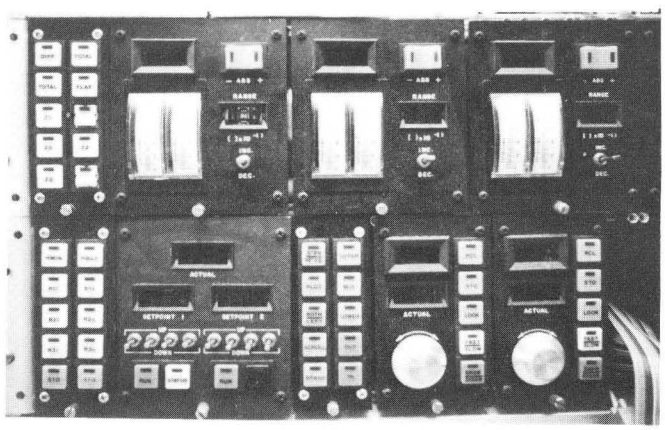

Fig. 22: A portion of the control console showing probe controls at left, slit and target current meters (top center and right) and magnetic bump controls for beam extraction (lower right). The dark rectangular frames on each module contain digital and alphanumeric display registers to show function values or to identify the elements but the red characters in them did not reproduce photographically.

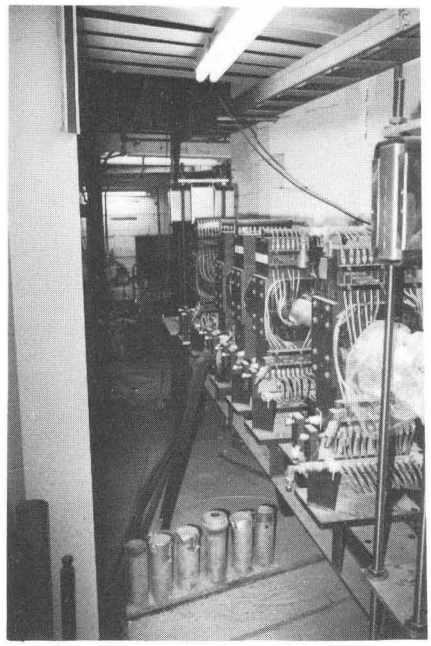

Fig. 23: External beam line leading to experimental areas. The cyclotron is being assembled in the bright area in the background.

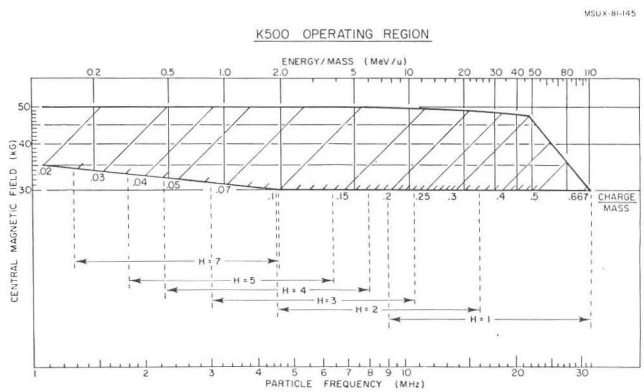

Fig. 24: Operating diagram for the K500 cyclotron showing the complete range of rf harmonic numbers and ion species needed for injector and stand-alone operation.